ISSN: 2754-4966

Journal of Nanosciences Research & Reports

SCIENTIFIC Research and Community

Research Article

Open Access

Enhanced Optical and Structural Properties of ZnSe Nanoparticles Synthesized by Pulsed Laser Ablation in Liquid

MA Jafarov*, AM Rahimli, SA Jahangirova, VU Mammadov and EF Nasirov

Baku State University, AZ1148, Zahid Khalilov Street 23, Baku, Azerbaijan

ABSTRACT

ZnSe nanoparticles, with applications in optoelectronic devices such as LEDs, solar cells, and photodetectors, were synthesized using pulsed laser ablation in liquid (PLAL)-a surfactant-free method that enables the production of high-purity nanoparticles with precise control over particle size and morphology. Laser ablation was performed using an Nd laser with a wavelength of 1064 nm, pulse energy of 135 mJ, and a pulse duration of 10 ns. X-ray diffraction confirmed the formation of hexagonal ZnSe nanocrystals, with an average crystallite size of 27.53 nm. Scanning electron microscopy (SEM), atomic force microscopy (AFM), and energy dispersive X-ray analysis (EDX) were used to characterize the nanoparticles' size, morphology, and stoichiometry. Absorption and photoluminescence spectra revealed a band gap of 3.30 eV and indicated excitonic emissions in the nanoparticles when excited by the second harmonic of the laser. These findings highlight PLAL as an effective technique for synthesizing ZnSe nanoparticles with controlled optical and structural properties, making them suitable for diverse applications in optoelectronics.

Corresponding author

MA Jafarov, Baku State University, AZ1148, Zahid Khalilov Street 23, Baku, Azerbaijan.

Received: February 26, 2025; **Accepted:** March 04, 2025; **Published:** March 12, 2025

Keywords: ZnSe Nanoparticles, Laser Ablation, Absorption, Luminescence

Introduction

Semiconductor nanoparticles have recently attracted significant attention due to their unique physical and chemical properties. Zinc selenide (ZnSe) is a particularly valuable material for optoelectronic applications, thanks to its wide band gap of 2.42 eV, which makes it suitable for use in luminescent screens, scintillation sensors, photodetectors, light-emitting diodes (LEDs), and solar cells [1-3]. Various methods for synthesizing ZnSe nanoparticles have been explored, including gas-dynamic, chemical, plasma, and radiation techniques [4-11]. Among these, pulsed laser ablation in liquid (PLAL) stands out as a promising method due to its simplicity and effectiveness [12-14].

Laser ablation in liquid has garnered interest for its ability to produce nanoparticles without the need for surfactants, allowing for superior control over size and shape. This method enables the tailoring of nanoparticle characteristics through various parameters, such as laser energy density, wavelength, pulse duration, and the type of colloidal solution. Notably, one of the key advantages of PLAL is its ability to synthesize pure nanoparticles, free from the contaminants often associated with chemical methods. The purity of these nanoparticles is crucial for their performance in numerous applications, as impurities can significantly affect their optical and electronic properties. Previous studies have reported that nanoparticles produced via laser ablation can grow through the coalescence of atoms and ions dispersed in the solution, highlighting the dynamic nature of this synthesis technique.

Pulsed laser ablation in liquid environments (PLAL) represents a novel approach to synthesizing nanostructures, offering advantages over conventional methods. This technique not only addresses issues of agglomeration and impurities but also provides a straightforward and cost-effective production system that does not require complex vacuum setups. The resultant nanostructures are efficiently collected in colloidal solutions, making them easy to handle in either suspension or powder form [15-17].

The mechanism behind the synthesis begins with the absorption of laser energy during its interaction with the target material. In semiconductors and insulators, light absorption predominantly occurs through resonant excitations of interband transitions. Photons with energy below the material's band gap are unlikely to be absorbed, making the understanding of the absorption spectra critical for optimizing synthesis conditions. In contrast, metals absorb laser light primarily through free electrons in the conduction band [18-21].

In this study, we propose a synthesis method for ZnSe nanoparticles using atoms from the starting material in an appropriate solution. This approach allows for a comprehensive analysis of the structural, surface morphology, and optical properties, accounting for the contributions of both the solvent and the nanoparticles. Our experimental findings reveal that the structural characteristics and optical properties of nanoparticles synthesized through PLAL significantly surpass those of nanoparticles derived from bulk crystals.

Furthermore, this work aims to address the deficiencies observed in existing studies by elucidating the impact of synthesis parameters on nanoparticle characteristics and demonstrating the enhanced

optical properties of ZnSe nanoparticles produced via PLAL. By refining the synthesis process, we hope to contribute valuable insights that will enhance the applicability of ZnSe nanoparticles in advanced optoelectronic technologies, ultimately positioning PLAL as a leading method for producing high-purity, controllable semiconductor nanoparticles.

Experimental Part

Synthesis of ZnSe Nanoparticles

All chemical reagents were used without preliminary purification: Zinc (Zn, 99.99% purity) and thiourea (SeO_2, 99.9% purity). ZnSe nanoparticles were synthesized by laser ablation of a solid target in a liquid medium. High-purity SeO_2 (99%) in a solution of distilled water was used as the starting material. The ablation process was carried out using laser radiation with a wavelength of $\lambda = 1064$ nm, pulse energy of 135 mJ, and an ablation time of approximately 10 minutes. A pulsed Nd laser with built-in generators for the 2nd and 3rd harmonics, designed to generate radiation at wavelengths of 1064, 532, and 355 nm, was used as the radiation source. The laser pulse duration was 10 ns, with a maximum power of approximately 12 MW/cm². The radiation intensity was varied using calibrated neutral density filters. Experiments show that nanosecond laser pulses cause material ablation through melting and evaporation, leading to the formation of a plasma plume of ablated particles at the point where the laser beam strikes the material surface. During irradiation, the plasma plume appears as a bright white spot. Nanoparticles are formed by nucleation in the vapor phase during the condensation of plasma plume particles due to adiabatic cooling.

Characterization of Nanoparticles

X-ray diffraction analysis was performed on a Rigaku MiniFlex 600 XRD diffractometer at ambient temperature. Cu Kα radiation from a Cu X-ray tube (operating at 15 mA and 30 kV) was used in all cases. The samples were scanned in the Bragg angle 2θ range of 20–70°. The morphology of the nanocomposites was analyzed using scanning electron microscopy (SEM). The SEM images were obtained with a Jeol JSM-767 F SEM in secondary electron imaging mode at a keV voltage, with a 4.5 mm distance between the sample and the electron probe. The energy dispersive X-ray spectrum (EDAX) was acquired using an SEM-X-Max 50 detector attached to the SEM. AFM analysis of the nanocomposites was performed on an NT-MDT Integra Prima atomic force microscope (Russia, Zelenograd) in semicontact mode, using specialized cantilevers with a gold coating (high-resolution semicontact silicon AFM cantilevers, NSG01 series, with a resonant frequency of 87–230 kHz and a force constant of 1.45–15.1 N/m). The optical absorption and luminescence spectra of ZnSe nanoparticles were studied using an automatic dual-dispersive monochromator (M833, with a spectral resolution of ~0.024 nm at a wavelength of 600 nm), controlled by a computer, and a detector that records radiation in the wavelength range of 350–2000 nm. The experimental setup is illustrated in Figure 1a.

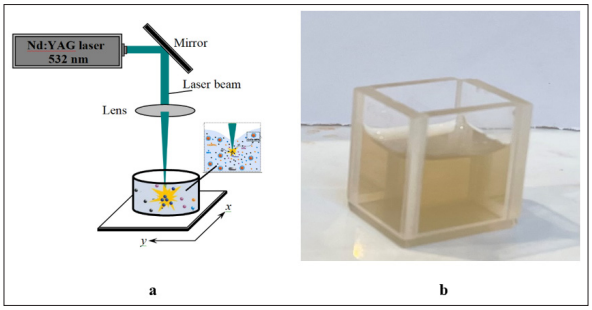

Figure 1: (a) Diagram of the Experimental Setup for the Ablation of ZnSe Nanoparticles in a Liquid Medium. (b) Colloidal Solution of ZnSe Obtained by Laser Ablation in a Liquid Medium

Results and Discussion

Following irradiation with laser pulses, ZnSe nanoparticles were promptly formed in the liquid medium. Notably, the color of the freshly prepared colloidal ZnSe suspension exhibited a dependence on the laser radiation flux density. Specifically, nanoparticles synthesized at lower laser energy densities produced a light yellow color, which transitioned to a darker yellow as the energy density increased (Figure 1b). This color change may be attributed to variations in the particle size of ZnSe in response to the energy density applied during the laser ablation process. To further elucidate the structural characteristics of these nanoparticles, X-ray diffraction (XRD) analysis was performed. Figure 2 presents the XRD pattern of nanoparticles collected from drops of the colloidal ZnSe solution that were dried on a clean glass substrate. The diffraction pattern reveals distinct peaks at 2θ values of 24.20° (100), 28.63° (002), 31.76° (101), 44.80° (110), 60.20° (103), and 74.00° (112), corresponding to the hexagonal phase of pure ZnSe nanocrystals present in the synthesized material. Based on the X-ray diffraction patterns, the sizes of the resulting nanoparticles were calculated using the Debye–Scherrer equation [22]:

$$D = k\lambda / \beta \cos \theta \qquad (1)$$

where D is the size of nanoparticles, k = 0.9 is the line shape coefficient (shape factor), β = 0.035 A0 is the half-width of the intensity maximum (FWHM - Full width at half maximum λ is the wavelength of X-ray radiation, λ = 1.54 Å, θ – Bragg angle, cos θ=0.727.

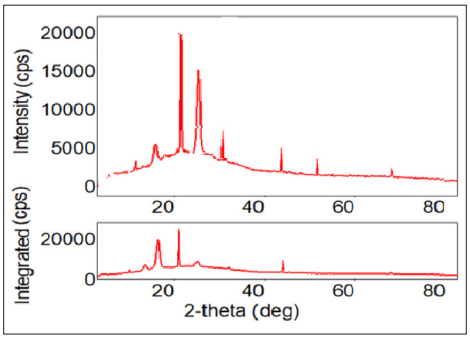

Figure 2: X-ray Diffraction Pattern (XRD) of ZnSe Nanoparticles Synthesized by Laser Ablation

The diffraction peaks of the as-prepared ZnSe samples at 2θ = 13.44°, 16.49°, 28.63°, 31.75°, 44.80°, and 53.52° correspond to the Miller indices (111), (220), (103), (202), (212), and (311), respectively. This is in accordance with data reported in the literature [20-22]. Therefore, the diffraction pattern can be indexed to the hexagonal structure of ZnSe. Estimates show that the average size of the ZnSe crystallites is approximately 29.53 nm (see Table 1).

Table 1: Sizes of ZnSe Crystallites Calculated Using the Debye Scherer Formula

2θ	Crystallite Size (nm)
24.20	51.45
28.63	36.75
31.75	37.25
44.80	16.86
53.52	5.7
72.60	31.45
Average Crystallite Size (nm)	29.53

Figure 3a presents an SEM image of ZnSe nanoparticles synthesized at varying laser radiation densities. It is evident that both the size and morphology of the nanoparticles are influenced by the laser radiation flux density. A diverse range of morphologies was observed, including spherical nanoparticles, monopod rods, bipod rods, and tripod rods. At low excitation intensities of 0.5 MW/cm², the average particle size was approximately 50 nm, with noticeable agglomeration. As the laser radiation flux density increased from 0.5 to 4 MW/cm², the nanoparticles evolved into multi-arm micro- and nanostructures, with arm lengths ranging from 1.7 to 4.9 μm and diameters between 90 and 300 nm. Further structural analysis of the ZnSe nanoparticles was conducted using energy dispersive X-ray spectroscopy (EDAX), which revealed a cadmium-to-sulfur ratio of 1:1 (see Figure 3b). This stoichiometric ratio indicates a balanced composition of the synthesized material.

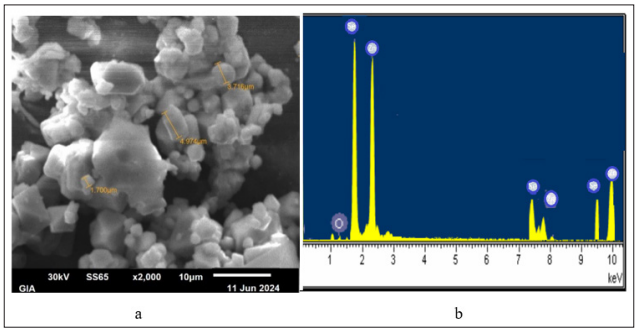

Figure 3: SEM Image (a) and EDAX Spectrum (b) of ZnSe Nanoparticles

To further characterize the synthesized nanoparticles, atomic force microscopy (AFM) analysis was performed. Figure 4a displays a three-dimensional AFM image of the ZnSe nanoparticles. As seen in the figure, homogeneous distribution of particles is not evident. The average particle size, estimated using the software, was approximately 70 nm. A histogram illustrating the nanoparticle size distribution is shown in Figure 4b. According to the histogram, the average size of the nanoparticles was estimated to be 60 nm. This size is larger than that calculated from X-ray diffraction (XRD) analysis, which can be attributed to the fact that XRD measurements reflect the free volume of dimensional defects, while AFM directly visualizes the particles without accounting for crystal defects [22]. The formation of larger particles may be explained by the aggregation of smaller particles.

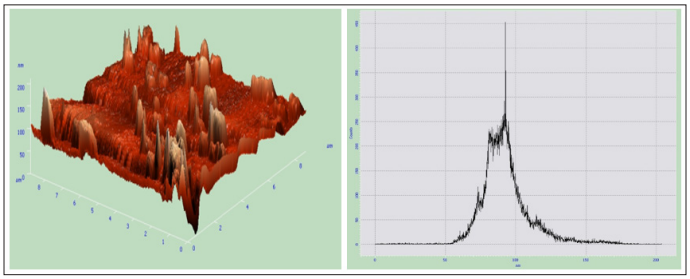

Figure 4: (a) AFM Image of ZnSe Nanoparticles and (b) Histogram of Size Distribution of ZnSe Nanoparticles

The optical properties of the synthesized ZnSe nanoparticles were further investigated through ultraviolet (UV) studies. The absorption curve of ZnSe nanoparticles is shown in Figure 5a. Since ZnSe is a semiconductor with a direct band gap, the band gap width of the studied samples was determined from the dependence of absorption on photon energy, resulting in a value of E_g=3.10eV (Figure 5b). This value is 0.38 eV larger than the bulk undoped ZnSe crystal (E_g=2.72eV).

The observed increase in the band gap of ZnSe nanoparticles to E_g=3.10eV is attributed to the quantum size effect, a common phenomenon in semiconductor nanostructures. As particle dimensions decrease, the confinement of charge carriers raises the energy required for electron transitions. This aligns with previous studies on various semiconductor nanoparticles synthesized using methods such as chemical vapor deposition and sol-gel techniques. The pulsed laser ablation method used in this study allows for precise control over nanoparticle size and morphology, enhancing the potential for optoelectronic applications, including UV photodetectors and light-emitting diodes (LEDs). The observed red shift in the absorption edge to shorter wavelengths, indicative of the quantum size effect, underscores the ability to engineer the band gap through size manipulation.

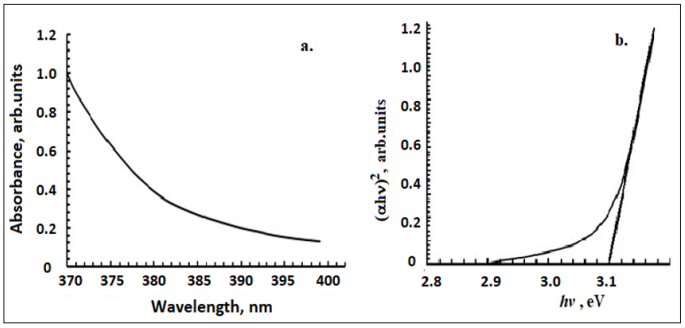

Figure 5: Optical Absorption Spectrum of ZnSe Nanoparticles (a) and the dependence of the absorption Coefficient on Photon Energy $\alpha^2 \sim f(h\nu)$ (b)

Figure 6a shows the photoluminescence spectra of ZnSe nanoparticles excited by the second harmonic of the N_d laser. The emission peak at approximately 405 nm (3.07 eV) is indicative of radiative recombination processes occurring within the material. The narrow full width at half maximum (FWHM) of the emission line, around 2 nm (~20 Å), suggests a high degree of uniformity in the energy levels of the emitting states, which is characteristic of well-defined excitonic transitions.

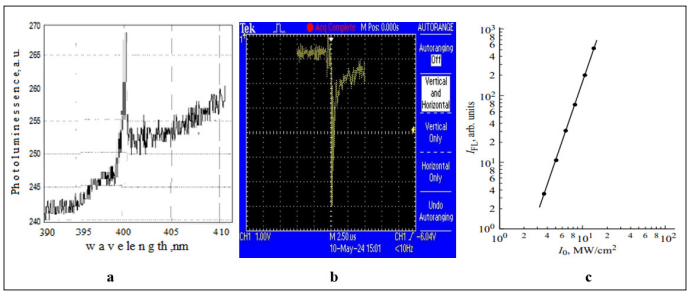

Figure 6: (a) Photoluminescence spectra of ZnSe nanoparticles excited by the Nd laser radiation.
(b) Photoluminescence relaxation curve of ZnSe. (c) Dependence of photoluminescence intensity (IPL) at the maximum wavelength (λ = 400 nm) against the laser intensity (Ilas)

The emission is attributed to free excitons, which are bound states of electrons and holes that can recombine to emit light. The energy of the free excitons in ZnSe is approximately 27 meV. Accounting for this energy, we deduce a band gap of 3.12 eV for the ZnSe nanoparticles, which is in good agreement with the value obtained from absorption spectrum analysis. This consistency reinforces the validity of the measurement techniques and the quality of the synthesized nanoparticles. The excitonic nature of the observed emission is further corroborated by the photoluminescence kinetics presented in Figure 6b. The rapid relaxation time of approximately 5×10^{-7} s is typical for excitonic

luminescence, suggesting that the recombination processes occur quickly, which is beneficial for applications in optoelectronic devices. Moreover, the PL spectra of thin ZnSe films demonstrate a pronounced increase in photoluminescence intensity with rising excitation intensities. This behavior is illustrated in Figure 6c, where the intensity of photoluminescence (I_{PL}) at the maximum wavelength (λ=400nm) is plotted against the laser intensity (I_{las}). The observed relationship, expressed as $I_{PL} \sim I_{las}^{3.3}$, indicates that at higher optical excitation levels, light amplification occurs. This phenomenon suggests that the thin ZnSe films could potentially be utilized in applications such as lasers and other light-emitting devices, where controlled amplification of light is essential. The emission is attributed to free excitons, which are bound states of electrons and holes that can recombine to emit light. The energy of the free excitons in ZnSe is approximately 27 meV. Accounting for this energy, we deduce a band gap of 3.12 eV for the ZnSe nanoparticles, which is in good agreement with the value obtained from absorption spectrum analysis. This consistency reinforces the validity of the measurement techniques and the quality of the synthesized nanoparticles.

The excitonic nature of the observed emission is further corroborated by the photoluminescence kinetics presented in Figure 6b. The rapid relaxation time of approximately 5×10^{-7} s is typical for excitonic luminescence, suggesting that the recombination processes occur quickly, which is beneficial for applications in optoelectronic devices.

Moreover, the PL spectra of thin ZnSe films demonstrate a pronounced increase in photoluminescence intensity with rising excitation intensities. This behavior is illustrated in Figure 6c, where the intensity of photoluminescence (IPL) at the maximum wavelength (λ=400nm) is plotted against the laser intensity (Ilas). The observed relationship, expressed as $I_{PL} \sim I_{las}^{3.3}$, indicates that at higher optical excitation levels, light amplification occurs. This phenomenon suggests that thin ZnSe films could potentially be utilized in applications such as lasers and other light-emitting devices, where controlled amplification of light is essential.

Conclusion

In this study, ZnSe nanoparticles were successfully synthesized via pulsed laser ablation in a liquid medium, with laser energy density playing a key role in controlling their size and morphology. X-ray diffraction confirmed the formation of hexagonal ZnSe, while scanning electron microscopy revealed diverse nanoparticle shapes, ranging from spherical to multi-arm structures. The photoluminescence spectra showed a strong emission peak at 400 nm, attributed to free exciton recombination, and a red shift in the band gap to 3.12 eV, consistent with the quantum size effect. These results demonstrate that pulsed laser ablation is an effective method for producing high-quality ZnSe nanoparticles with tunable optical properties. The ability to control particle size and morphology makes this approach promising for optoelectronic applications such as photodetectors, LEDs, and lasers.

References

1. P Gupta, RG Solanki, P Patel, KM Sujata, R Kumar, et al. (2023) Enhanced antibacterial and photoluminescence activities of ZnSe nanostructures. ACS Omega 8: 13670-13679.
2. AG Kyazim Zade, VM Salmanov, AG Guseinov, MA Jafarov (2019) Enhanced optical properties of ZnSe nanostructures. Chalcogenide Lett 16: 465-469.
3. HS Hong, MS Kim, EK Byun, YL Lee (2020) Facile synthesis and characterization of zinc selenide nanoparticles in aqueous solution at room temperature. J Cryst Growth 535: 125523.
4. M Imran, A Saleem, NA Khan, AA Khurram, N Mehmood (2018) Amorphous to crystalline phase transformation and band gap refinement in ZnSe thin films. Thin Solid Films 648: 31-38.
5. VM Salmanov, AG Guseinov, MA Jafarov, RM Mamedov, FSh Akhmedova, et al. (2024) Structural properties of ZnSe nanostructures. Russ J Phys Chem A 98: 1-5.
6. VM Salmanov, AG Guseinov, MA Jafarov, RM Mamedov, TA Mamedova (2022) Optical properties of ZnSe nanoparticles. Opt Spectrosc 130: 1308-1311.
7. MA Jafarov, EF Nasirov, AH Kazımzade, SA Jahangirova (2021) Synthesis and characterization of ZnSe nanoparticles. Chalcogenide Lett 18: 791-795.
8. ASh Abdinov, MA Jafarov, EF Nasirov, SA Jahangirova (2019) Nanotechnologies in Russia. Nanotechnol Russ 14: 185-189.
9. P Kumar, J Singh, MK Pandey, CE Jeyanthi, R Siddheswaran, et al. (2014) Synthesis, structural, optical, and Raman studies of pure and lanthanum-doped ZnSe nanoparticles. Mater Res Bull 49: 144-150.
10. AR Khezripour, D Souri, H Tavafi, M Ghabooli (2019) Serial dilution bioassay for antibacterial potential of ZnSe quantum dots and their Fourier transform infrared spectroscopy. Measurement 148: 106939.
11. D Souri, N Salimi, M Ghabooli (2021) Hydrothermal fabrication of pure ZnSe nanocrystals and their antibacterial potential. Inorg Chem Commun 123: 108345.
12. Irshad Ahmad Mir, Hammad Alam, Eepsita Priyadarshini, Ramavatar Meena, Kamla Rawat, et al. (2018) Antimicrobial and biocompatibility of ZnSe core and ZnSe/ZnS core-shell quantum dots. J Nanopart Res 20: 1-11.
13. AG Kyazym Zade, M Karabulur, AK Dincher, VM Salmanov, MA Dzhafarov (2019) Nanotechnologies in Russia. Nanotechnol Russ 10: 794-801.
14. MA Jafarov, EF Nasirov, AH Kazımzade, SA Jahangirova (2021) Optical properties of ZnSe nanostructures. Chalcogenide Lett 18: 791-795.
15. VM Salmanov, MA Jafarov, AG Guseinov, RM Mamedov, AA Salmanova (2021) Effect of synthesis parameters on the properties of ZnSe nanoparticles. Chalcogenide Lett 18: 155-159.
16. MA Jafarov, EF Nasirov, SA Jahangirova (2021) Synthesis of ZnSe nanoparticles using PLAL. J Optoelectron Adv Mater 21: 605-608.
17. J Archana, M Navaneethan, T Prakash, S Ponnusamy, C Muthamizhchelvan, et al. (2013) Chemical synthesis and functional properties of magnesium-doped ZnSe nanoparticles. Mater Lett 100: 54-57.
18. SY Bu, LW Li, P Xie, H Liu, SL Xue (2016) Synthesis and optical properties of ZnSe micro-grasses and microspheres grown on graphene oxide sheets by the hydrothermal method. Ceram Int 42: 5075-5081.
19. B Feng, J Cao, J Yang, S Yang, D Han (2014) Characterization and photocatalytic activity of ZnSe nanoparticles synthesized by a facile solvothermal method, and the effects of different solvents on these properties. Mater Res Bull 60: 794-801.
20. MR Kim, JH Chung, M Lee, S Lee, DJ Jang (2010) Fabrication, spectroscopy, and dynamics of highly luminescent core-shell InP/ZnSe quantum dots. J Colloid Interface Sci 350: 5-9.
21. G Lu, H Ana, Y Chen, J Huang, H Zhang, et al. (2005) Temperature dependence of Raman scattering of ZnSe nanoparticle grown through vapor phase. J Cryst Growth

274: 530-535.

22. R Hernández, E Rosendo, G García, M Pacio, T Díaz, et al. (2014) Obtaining and characterization of ZnSe nanoparticles from aqueous colloidal dispersions. Superficies y Vacío 27: 11-14.